Recent trends in the chemistry of major northern rivers signal widespread Arctic change

Suzanne Tank, James Mcclelland, Robert Spencer, Alexander Shiklomanov, Anya Suslova, Florentina Moatar, Rainer Amon, Lee Cooper, Greg Elias, Vyacheslav Gordeev, et al.

Long-term Trends in Arctic Riverine Chemistry Signal Multi-faceted Northern Change

Suzanne Tank (suzanne.tank@ualberta.ca)
University of Alberta https://orcid.org/0000-0002-5371-6577

James McClelland
Marine Biological Laboratory

Robert Spencer
Florida State University

Alexander Shiklomanov
University of New Hampshire

Anya Suslova
Woodwell Climate Research Center

Florentina Moatar
INRAE

Rainer Amon
Texas A&M University, Galveston Campus https://orcid.org/0000-0002-1437-4316

Lee Cooper
University of Maryland

Greg Elias
Western Arctic Research Center

Vyacheslav Gordeev
Russian Academy of Sciences

Christopher Guay
Mamala Research LLC

Tatiana Gurtovaya
South Russia Centre for Preparation and Implementation of International Projects

Lyudmila Kosmenko
Ministry of Natural Resources and Environment of the Russian Federation

Edda Mutter
Yukon River Inter-Tribal Watershed Council

Bruce Peterson
Marine Biological Laboratory

Bernhard Peucker-Ehrenbrink
Woods Hole Oceanographic Institution https://orcid.org/0000-0002-3819-992X

Peter Raymond

Yale University https://orcid.org/0000-0002-8564-7860
Paul Schuster
U.S. Geological Survey https://orcid.org/0000-0002-8314-1372
Lindsay Scott
Woodwell Climate Research Center
Robin Staples
Government of the Northwest Territories
Robert Striegl
US Geological Survey https://orcid.org/0000-0002-8251-4659
Mikhail Tretiakov
Arctic and Antarctic Research Institute https://orcid.org/0000-0003-3702-6362
Alexander Zhulidov
South Russia Centre for Preparation and Implementation of International Projects
Nikita Zimov
Northeast Science Station
Sergey Zimov
Northeast Science Station of Pacific Geographical Institute https://orcid.org/0000-0002-0053-6599
Robert Holmes
Woodwell Climate Research Center

Article

Keywords:

Posted Date: February 9th, 2023

DOI: https://doi.org/10.21203/rs.3.rs-2530682/v1

Additional Declarations: There is **NO** Competing Interest.

Version of Record: A version of this preprint was published at Nature Geoscience on August 21st, 2023.
See the published version at https://doi.org/10.1038/s41561-023-01247-7.

Long-term Trends in Arctic Riverine Chemistry Signal Multi-faceted Northern Change

Suzanne E. Tank[1], James W. McClelland[2], Robert G.M. Spencer[3], Alexander I. Shiklomanov[4], Anya Suslova[5], Florentina Moatar[6], Rainer M.W. Amon[7], Lee W. Cooper[8], Greg Elias[9], Vyacheslav V. Gordeev[10], Christopher Guay[11], Tatiana Yu. Gurtovaya[12], Lyudmila S. Kosmenko[13], Edda A. Mutter[14], Bruce J. Peterson[2], Bernhard Peucker-Ehrenbrink[15], Peter A. Raymond[16], Paul F. Schuster[17], Lindsay Scott[5], Robin Staples[18], Robert G. Striegl[17], Mikhail Tretiakov[19], Alexander V. Zhulidov[12], Nikita Zimov[20], Sergey Zimov[20], Robert M. Holmes[5]

[1] Department of Biological Sciences, University of Alberta, Edmonton, AB, Canada
[2] Ecosystems Center, Marine Biological Laboratory, Woods Hole, MA, USA
[3] Department of Earth, Ocean and Atmospheric Science, Tallahassee, FL, USA
[4] Earth Systems Research Center, University of New Hampshire, Durham, NH, USA
[5] Woodwell Climate Research Center, Falmouth, MA, USA
[6] RiverLy, Centre de Lyon-Grenoble Auvergne-Rhône-Alpes, INRAE, Villeurbanne, France
[7] Department of Marine and Coastal Environmental Sciences, Texas A&M University, Galveston, TX, USA and Department of Oceanography, Texas A&M University, College Station, TX, USA
[8] Chesapeake Biological Laboratory, University of Maryland Center for Environmental Science, Solomons, MD, USA
[9] Western Arctic Research Center, Inuvik, NT, Canada
[10] Shirshov Institute of Oceanology, Russian Academy of Sciences, Moscow, Russian Federation
[11] Mamala Research LLC, Honolulu, HI, USA
[12] South Russia Centre for Preparation and Implementation of International Projects, Rostov-on-Don, Russian Federation
[13] Hydrochemical Institute of the Federal Service for Hydrometeorology and Environmental Monitoring, Ministry of Natural Resources and Environment of the Russian Federation, Rostov-on-Don, Russia
[14] Yukon River Inter-Tribal Watershed Council, Anchorage, AK, USA
[15] Marine Chemistry and Geochemistry Department, Woods Hole Oceanographic Institution, Woods Hole, MA, USA
[16] School of Forestry & Environmental Studies, Yale University, New Haven, CT, USA
[17] U. S. Geological Survey, Earth System Processes Division, Boulder, CO, USA
[18] Water Resources Division, Government of the Northwest Territories, Yellowknife, NT, Canada
[19] River Estuaries and Water Resources Department, Arctic and Antarctic Research Institute, Saint Petersburg, Russian Federation
[20] Pacific Geographical Institute of the Far Eastern Branch of the Russian Academy of Sciences, Chersky, Russian Federation

Abstract

Large rivers integrate processes occurring throughout their watersheds, and are therefore sentinels of change across broad spatial scales. Riverine chemistry also regulates ecosystem function across Earth's land-ocean continuum, exerting control from the micro- (e.g., food web) to the macro- (e.g., carbon cycle) scale. In the rapidly warming Arctic, a wide range of processes have been hypothesized to alter river water chemistry. However, it is unknown how the land-ocean flux of waterborne constituents is changing at the pan-Arctic scale. Here, we show profound shifts in the concentration and transport of biogeochemical constituents in the six largest Arctic rivers (the Ob', Yenisey, Lena, Kolyma, Yukon, and Mackenzie) since 2003, near river mouths capturing two-thirds of the pan-Arctic watershed. While some constituent fluxes increase substantially at the pan-Arctic scale (alkalinity and associated ions), others decline (nitrate and associated inorganic nutrients) or are overall unchanged (dissolved organics). These clear but divergent trends diagnose a multi-systems perturbation that indicates alteration of processes ranging from chemical weathering on land, to primary production in the coastal ocean. We anticipate these findings will refine models of current and future functioning of the coupled land-ocean Arctic system, and spur research on scale-dependent change across the river-integrated Arctic domain.

Main

Large rivers are planetary linchpins, connecting vast swaths of terrestrial landmass to the world's coastal oceans. On land, rivers integrate patchy landscapes and the variable biogeochemical processes that these landscapes host, as water moving through watersheds incorporates the chemical signature of its flow path. In the coastal ocean, the chemical signature of water transported by rivers regulates nearshore biogeochemical[1,2] and ecological[3,4] function; over broader scales, river water and its composition modify ocean physics[1]. Nowhere is this more consequential than in the Arctic, where ~11% of Earth's riverine discharge drains into an enclosed basin containing ~1% of global ocean volume[5]. This drainage occurs predominantly via six large rivers (Figure 1, Extended Data Table 1). As a result, quantifying trends in river water chemistry at a constrained series of downstream sites allows us to diagnose change across much of the pan-Arctic watershed, better understand the current functioning of the connected land-ocean Arctic system, and predict what the future may hold for this rapidly changing region[6].

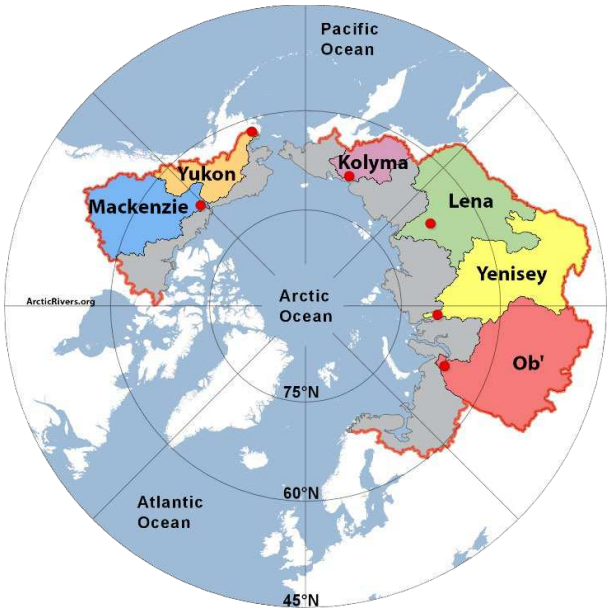

Figure 1: The six great Arctic rivers that are the focus of this assessment. Sampling locations are indicated by red dots. The 16.8 x 10^6 km^2 pan-Arctic watershed is delineated by the red line.

Past work on north-flowing rivers has established significant increases in discharge across the pan-Arctic since the early-mid 20th century[7,8] (Figure 2), attributed to intensification of the hydrologic cycle[9]. Such increases in water transport suggest that we should expect long-term change in the riverine flux (i.e., total riverine transport, as mass $time^{-1}$) of biogeochemical constituents, particularly for constituents such as organic carbon that are transport, rather than supply, limited in the north[10,11]. Similarly, there is a broadly articulated expectation that permafrost thaw will increase the transport of organic matter, nutrients, and ions to aquatic networks, and thus their delivery to the coastal ocean[12-14]. However, these assessments miss that change in the north is multi-faceted, with factors such as shrubification[15], temperature-induced increases in biogeochemical processing rates by heterotrophic and autotrophic microbes[16-18], disturbances such as wildfire[19], and human modifications such as river impoundment[20-22], changing land use[23], and changing industrial emissions[24] often occurring simultaneously, with the potential for antagonistic effects[e.g., 25]. Even for permafrost thaw, deepening flowpaths[26] or processes such as sorption[27,28] can lead to patterns in mobilization that vary between sites or regions[29].

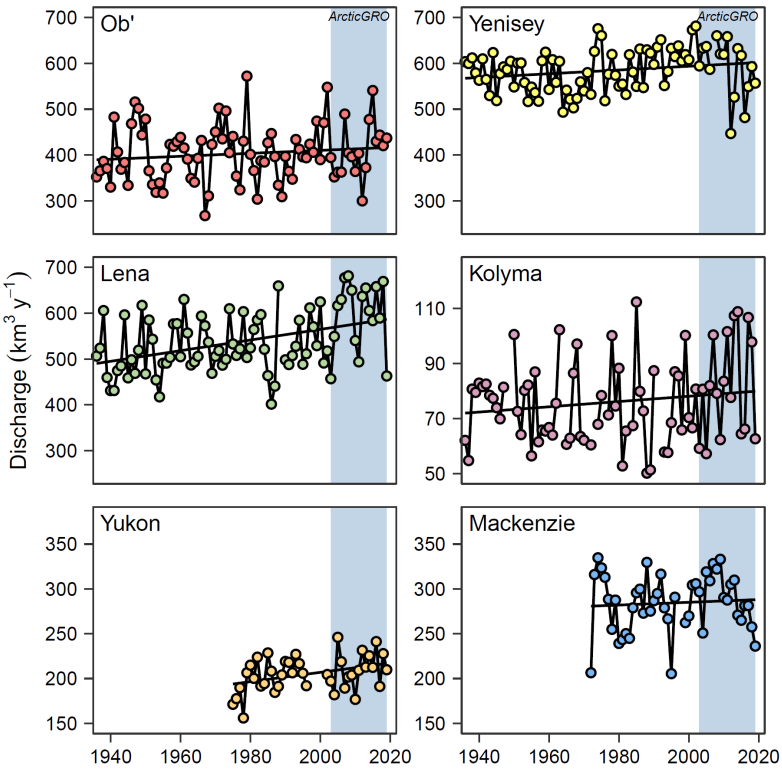

Figure 2: Long-term discharge record for each of the six great Arctic rivers. The timespan of the ArcticGRO data record is indicated with blue shading.

Here, we examine a nearly twenty-year record of coupled river discharge and chemistry (Extended Data Figure 1) collected from the six largest rivers that drain to the Arctic Ocean. These rivers: the Ob', Yenisey, Lena, and Kolyma in Russia, and the Mackenzie and Yukon in North America, capture two-thirds of the Arctic Ocean watershed area (Figure 1, Extended Data Table 1). This data record is the result of our group's ongoing efforts via the Arctic Great Rivers Observatory (ArcticGRO; www.arcticgreatrivers.org), which — given the challenge of collecting methodologically-consistent and seasonally-representative samples across these diverse jurisdictions and sites — represents an unparalleled resource for exploring Arctic riverine change. Our analyses reveal trends at magnitudes that signal broad-scale perturbation throughout the pan-Arctic, but with divergent trajectories that shed light on variable mechanisms of change. We use these insights to consider potential drivers of effect and

the consequences of observed change, and to explore where knowledge gaps are hampering our ability to understand current and future functioning of the land-ocean Arctic system.

Pronounced, but divergent trends in Arctic riverine flux

We focus our assessment on three chemical constituents that are important drivers of biogeochemical function across the land-ocean Arctic domain, and that are also representative of broader constituent classes. These are: dissolved organic carbon (DOC; representative of the broader organic matter pool including organic-associated nutrients); alkalinity (representative of many dissolved ions); and nitrate (NO_3^-; representative of dissolved inorganic nutrients, including ammonium (NH_4^+) and silica (SiO_2)) (Extended Data Figure 2). To assess constituent flux, we applied a modelling approach that couples daily discharge data with more sporadic concentration measurements, and makes use of the known relationship between concentration and discharge to determine flux (*see Methods*)[30]. Of our focal suite, only alkalinity experienced a pan-Arctic (i.e., six rivers combined) increase in annual flux over our period of record (Figure 3a). Nitrate declined significantly, while DOC, which has often been a focus of study given its role as a rapid-cycling component of the contemporary carbon cycle, showed no discernable change at the pan-Arctic scale (Figure 3b-c). Change that did occur, however, was substantial, with a 32% decline in NO_3^- and an 18% increase in alkalinity over a period of 17 years. An assessment of trends in flux across the broad suite of constituents measured by the ArcticGRO program (Extended Data Figure 3) reveals patterns within constituent classes (i.e., Extended Data Figure 2) that generally track those for the focal constituents. For example, trends in flux for ions closely affiliated with alkalinity (Ca^{2+}, Mg^{2+}, Li^+, Sr^{2+}) largely tracked that constituent; nutrients (SiO_2 and NH_4^+) showed a pan-Arctic decline similar to that for NO_3^-; and patterns for total dissolved phosphorus were similar to those for DOC. Given that these constituents are regulated by processes ranging from chemical weathering[2] to biological uptake[16-18] on land; and modify processes ranging from ocean acidification[31] to primary

production[4] in the coastal ocean, the ecological and biogeochemical ramifications of the changes we observe are likely profound.

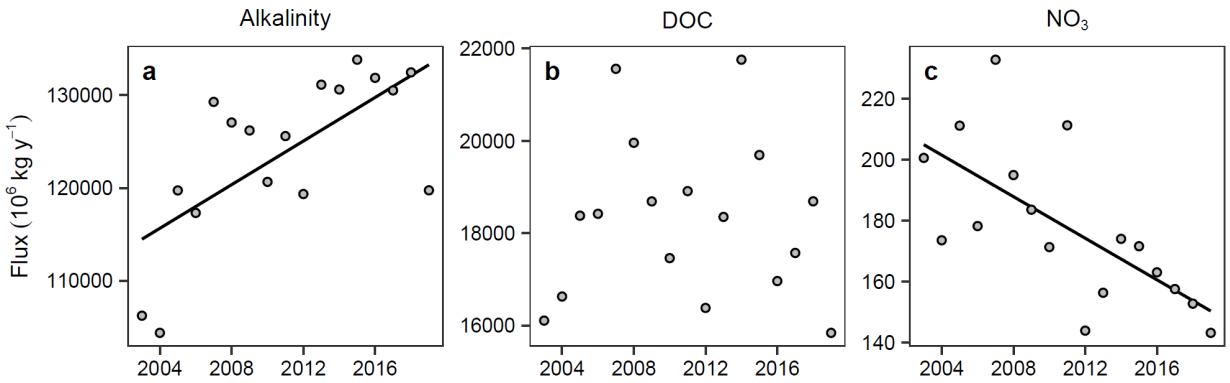

Figure 3: Trends in annual constituent fluxes of alkalinity (as $CaCO_3$), dissolved organic carbon (DOC), and nitrate (as NO_3-N), summed across the six great Arctic rivers. Fluxes are provided as 10^6 kg y^{-1}. Thiel-Sen slopes with $p<0.05$ are indicated as lines within each panel. Statistical outputs are provided in Table S1.

Concentration and discharge direct changing flux

In some cases, river-specific trends in constituent flux deviated from the pan-Arctic sum. For example, NO_3^- increased modestly in the Yukon ($p=0.12$), and showed little change in the Ob' ($p=0.70$) despite the pan-Arctic decline described above; alkalinity patterns for the Mackenzie (negative trend slope; $p=0.54$) contrasted with clear increases elsewhere; and DOC increased in the Ob' and decreased in the Yenisey ($p<0.02$) in the face of limited change in other rivers ($p=0.23$–0.84); (Figure 4a). In part, these patterns appeared to be driven by river-specific trends in discharge, which decreased in the Mackenzie ($p=0.02$) and Yenisey ($p=0.09$) over the 17-year length of our data record (Figure 4b) despite the longer-term increase in discharge documented for the pan-Arctic domain[7,8] (Figure 2). Examining the mechanisms underlying these changes in constituent flux requires that we disentangle inter-annual and long-term change in water discharge from co-occurring trends in concentration. This task is complicated by the fact that constituent concentrations vary seasonally and with discharge itself. We use two distinct approaches to resolve these two known concerns.

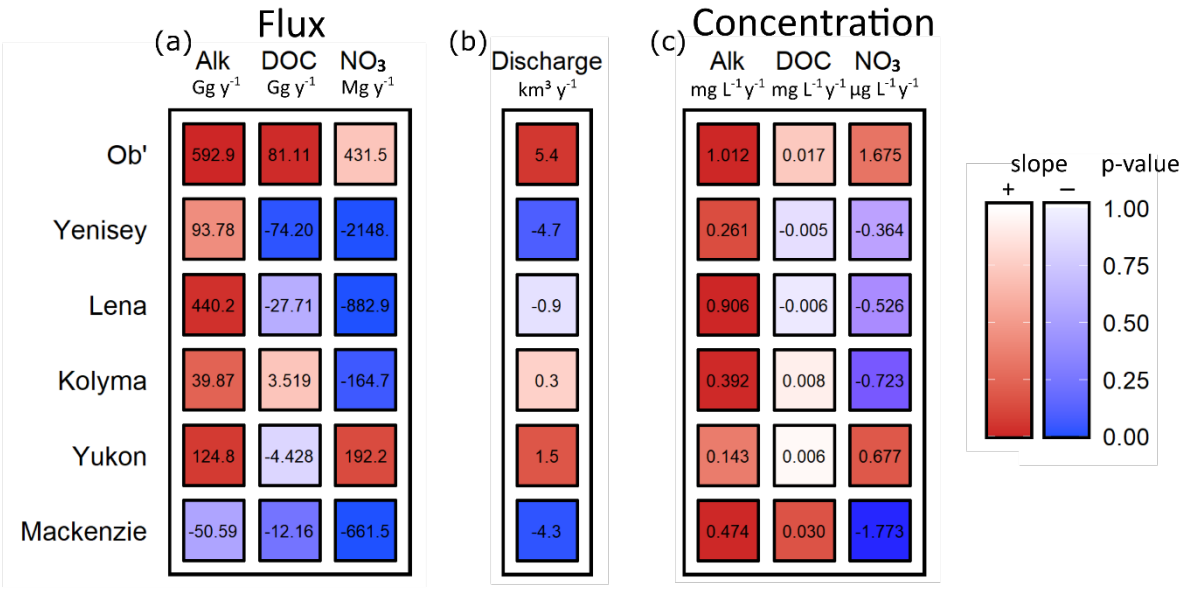

Figure 4: Annual trends for: (a) constituent flux; (b) discharge; and (c) concentration for each of the six great Arctic rivers. In each panel, the Sen's slope (numerical value) and p-value of the trend (shading) are shown. Flux and concentration trends for the full ArcticGRO constituent list are shown in Extended Data Figures 3 and 5, respectively; detailed statistical outputs are provided in Tables S1 and S2.

First, we use an approach to directly examine trends in measured concentrations, via trend analyses that are binned by season to account for seasonal variation in concentration unrelated to directional change over time (see *Methods*). We target this approach specifically to account for changes to the within-year seasonality of sampling across the two-decade timespan of the ArcticGRO program. Results from this direct trend analysis for concentration (Figure 4c) are generally similar to those for flux, described above (Figure 4a). Increases in alkalinity are widespread (p=0.00–0.14 in all rivers except the Yukon), nitrate concentrations decline (albeit modestly) across most rivers, and trends for DOC concentration are largely absent (p=0.73–0.96) in all rivers except for the Mackenzie, where DOC concentration increases modestly over time (p=0.16).

Second, we assess changes in flux controlled for inter-annual variation in discharge via a flow-normalization modelling approach that removes variation in discharge across years, but retains within-year (i.e., day-to-day) seasonality. Although this method does not generate an estimate of "true" flux, it is preferred when the analytical emphasis is mechanistic in nature (*see also Methods*)[32], because it

overcomes year-to-year fluctuations in discharge that can obscure underlying change. These flow-normalized fluxes show trends that largely reflect those for concentration presented above (Figure 4c), with some notable refinements: increases in alkalinity and decreases in NO_3^- become more robust, and a decrease in DOC emerges for the Kolyma while the DOC increase in the Mackenzie is maintained (Extended Data Figure 4). Overall, patterns for flow-normalized fluxes are remarkably similar to our best estimates of true flux and concentration presented above, with broad-scale increases in alkalinity and declines in NO_3^-, and variable and modest trends for DOC. Taken as a whole, these broad but divergent trends diagnose a multi-systems perturbation to the pan-Arctic system, with effects profound enough to reach the mouths of large northern rivers.

Divergent trends diagnose multi-systems change

The array of factors that might reasonably enable long-term change in riverine chemistry is diverse, varying regionally in magnitude and across chemical constituents in effect (Figure 5, Supplemental Text). As just one example, abrupt permafrost thaw (i.e., thermokarst) is a regionally-specific phenomena dependent on the presence of ground ice[33] that is generally understood to increase the transport of some constituents to riverine networks (e.g., inorganic nutrients)[29], but potentially decrease others (e.g., DOC, in cases where landscape collapse increases mineral sorption, or diverts hydrologic flow paths through mineral soils)[34,35]. As a result, the variation in response that we describe above can be used to diagnose drivers of change, and develop approaches to assess future functioning of the land-ocean Arctic system.

For some chemical constituents, known factors of change are both relatively widespread and consistent in their directionality (Figure 5; Supplemental Text). In the case of alkalinity and related ions, for example, exposure to deeper soils via either active layer deepening or thermokarst-associated permafrost thaw will typically increase mineral weathering by increasing water contact with deeper

mineral soils[36,37]. Acting synergistically, shrubification[38] and increased temperature-driven organic matter processing[39] will increase weathering rates via processes such as increasing soil pore water acidity. Because these processes are coherent in their directionality and geographically widespread, the net result appears as a cohesive increase in concentration and flux throughout the pan-Arctic domain.

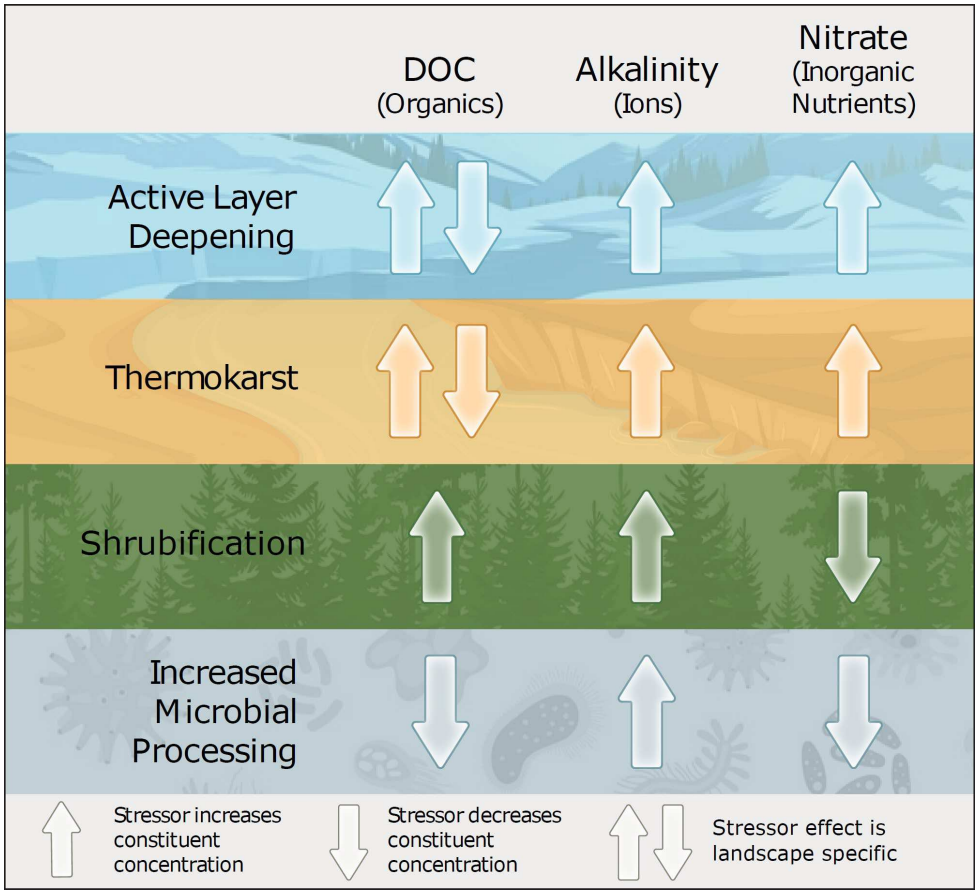

Figure 5: A conceptual diagram to illustrate key drivers of change of Arctic riverine chemistry, and their anticipated direction of effect for each of the three focal constituents. The Supplemental Text provides an overview of the literature evidence for this conceptual exercise, in addition to a description of drivers that are regional in their effect, or exert control largely outside of the timespan of the ArcticGRO data record.

For other constituents, variation in the directionality of factors of change appears to cause a muted overall response. In the case of DOC, for example, permafrost thaw can either increase[40] or decrease[34] loading to aquatic systems, depending on the composition of soils subject to thaw[35]. While greening will increase vegetation and litter substrates for leaching and therefore the transport of organic matter to aquatic networks[41], temperature-driven increases in mineralization[18,42] and potential

rapid processing of novel organic matter substrates[43] act in opposition to this effect. Across these large Arctic rivers, the net result appears to be a dissipation of effect with transport through aquatic networks, and little net change in DOC delivery to the coastal ocean over the timespan of this assessment.

Finally, in some cases, geographically widespread processes appear to overwhelm counteracting drivers. For example, although we broadly expect permafrost thaw to increase inorganic nitrogen delivery to aquatic networks[29], our analyses reveal declines in the transport of NO_3^- (and other inorganic nutrients) to the Arctic Ocean from large Arctic rivers. This suggests that factors such as temperature-driven increases in nitrogen cycling[17] or nitrogen uptake and/or immobilization[16,44] may currently be overwhelming local increases in mobilization[29], when assessed at the large-river watershed scale. These findings underline the importance of taking a systems approach to understanding Arctic change, with an acknowledgement that biogeochemical cycles are inherently linked across elements and space.

Broad perturbation in linked biogeochemical cycles across the land-ocean Arctic domain

Our analyses diagnose changes to the land-ocean Arctic system that are pervasive enough to leave few biogeochemically-active elements unscathed. As a result, these findings likely signal domain-scale change to ecosystem function. On land, ecosystem models have predicted increases in organic matter loading to fluvial networks in the changing north[45]. The lack of this signal at river outflows, therefore, suggests possible increases in carbon mineralization and associated outgassing during transit through watersheds, and thus an acceleration in carbon cycling within Arctic fluvial networks. Increasing alkalinity is suggestive of increases in chemical weathering, but in a region where a predominance of carbonate over silicate weathering, coupled with substantial sulfide oxidation in some watersheds, causes the ratio of CO_2 consumption: alkalinity generation to be overall low relative to the global mean[2]. Increasing SO_4 fluxes in rivers where SO_4 appears to be largely derived from sulfides (Extended Data

205 Figure 3; Yukon, Kolyma[46]) may in fact indicate increasing bicarbonate liberation in the absence of CO_2
206 fixation[2].

207 In the coastal ocean, riverine inputs of DIC result in CO_2 outgassing to the atmosphere[47]. The
208 magnitude of this effect relative to weathering-induced CO_2 fixation on land, and its change, will play a
209 key role in determining the carbon balance of the Arctic system. Acting concurrently, the declining NO_3^-
210 that we document is consistent with negative feedbacks for Arctic Ocean biological productivity and CO_2
211 uptake from the atmosphere, which is generally thought to be increasing as seasonal sea ice declines
212 and nutrients become more available[48]. However, the Arctic Ocean also has globally low N:P ratios
213 because its shelf sediments are a significant nitrogen sink through denitrification[49]. As a result,
214 decreases in riverine NO_3^- transport coupled with increasing discharge will increase stratification and
215 decrease availability of nutrients for biological production. The changes will play out alongside other co-
216 occurring processes, such as changes to the dilution effect of river water on ocean pH[2] with increasing
217 alkalinity, and consequent effects of this change on primary production[50].

218

219 **Conclusions**

220 In addition to implications for the current and future functioning of the land-ocean Arctic
221 system, our findings point to several important considerations for understanding change. Particularly for
222 bio-reactive constituents (DOC, nutrients), this work illustrates the importance of scale. Widespread
223 declines in constituents such as NO_3^- in the face of local processes known to increase land-water
224 mobilization suggests a fulcrum-like redistribution in biogeochemical cycling at the landscape-scale,
225 where fine-scale uptake and processing is increasing at the expense of communities downstream. How
226 the balance between local mobilization and broader-scale processing may shift for the smaller
227 catchments encircling the Arctic Ocean that have much shorter in-river transit times (see, for example,
228 NO_3^- trends in refs. [51,52]), or for other bio-reactive constituents (dissolved organic matter and other

inorganic nutrients) remains an open question. However, this potential scale-dependent variation in river mouth trends will be an important determinant of the geographic distribution of change in the Arctic nearshore. Teasing apart the relative importance of various drivers of change, and how they will vary with time and across constituents, will require process-based models, as already developed for alkalinity[39] and DOC[45], in addition to models that are linked across elements and space[47]. These models must inherently co-consider multiple drivers of change, including those not directly discussed above (e.g., impoundment, declining acid deposition, land use and land cover change; see also Supplemental Text). The datasets we draw on for our analyses are remarkable for their geographic cohesion and their relative length. However, they also diagnose profound change occurring in real time. This work clearly calls for continued, coordinated observation of the land-ocean Arctic system. More importantly, however, it reinforces the need for rapid attention to Earth's warming climate, and its multiplicative effects in the north.

Online Methods

Sample collection and dataset coverage

Water chemistry: We began sampling the six largest Arctic rivers for water chemistry in the summer of 2003. The project was initially called PARTNERS (Pan-Arctic River Transport of Nutrients, Organic Matter, and Suspended Sediments), and was expanded and renamed the Arctic Great Rivers Observatory (ArcticGRO) in 2008. Sample collection for the data presented in this paper occurred 5-7 times per year, with the exception of a short break during 2007-08 (Extended Data Figure 1). Water chemistry samples are collected as far downstream on each of the six Great Arctic rivers as logistically feasible, at Salekhard (Ob'), Dudinka (Yenisey), Zhigansk (Lena), Cherskiy (Kolyma), Pilot Station (Yukon), and Tsiigehtchic (Mackenzie) (Figure 1; Extended Data Table 1). Between 2003 and 2011, open water sampling was conducted using a D-96 sampler[53] equipped with a Teflon nozzle and Teflon sample collection bag, which enabled depth-integrated and flow-weighted samples. Samples were collected at five roughly equal increments across the river channel and combined in a 14-L Teflon churn, resulting in a single composite sample. Beginning in 2012, open-water sampling was conducted by collecting three near-surface samples on each of the left-bank, right-bank, and mid-points of each river, and combining these to form a composite sample. Across the full period of record, wintertime (under ice) samples were collected by drilling a hole at the river's mid-point, and collecting a sample from below the ice surface.

Within years, the timing of sample collection has changed slightly over the ArcticGRO period of record. Early collection schemes (2003-06 and 2009-11) focused on the spring freshet (three or more samples

per year), with further sample coverage through the more broadly-spread late summer (period of deepest thaw of the seasonally-frozen active layer; one to four samples) and winter (typically one sample) periods. Given the paucity of cross-site comparable data for these rivers at the outset of the ArcticGRO program, this sampling scheme was designed to maximize coverage during the high flows of the spring, when constituent concentrations are changing rapidly and the majority of constituent flux occurs[54]. In 2012, sampling shifted to become evenly spread across the annual cycle, with samples collected bi-monthly (i.e., six samples per year), and months of collection alternating between years. Sample processing (i.e., filtering and preservation) occurs within 24 hours of sample collection. As described above for sample collection, processing protocols were identical across all sites. Processed and preserved samples were shipped to Woods Hole, MA, where they were distributed to specialized laboratories for individual analyses. A complete description of processing and analytical methodologies is available on the ArcticGRO website (www.arcticgreatrivers.org), and archived at the Arctic Data Center[55]. The focal constituents highlighted in this paper were analyzed as follows: For DOC, on a Shimadzu TOC analyzer, following acidification with HCl, sparging, and using the 3 of 5 injections that resulted in the lowest coefficient of variation; for alkalinity, following acid titration using a Hach digital titrator (2003-2009) and Mettler Toledo model T50M titrator (2010 onwards); for NO_3^- (as $NO_3^- + NO_2^-$) colorimetrically using a Lachat Quickchem FIA+ 8000 (2003-2011) and Astoria (2012 onwards) autoanalyzer.

Discharge: All Arctic-GRO discharge measurements are from long-term gauging stations operated by Roshydromet, the US Geological Survey, and the Water Survey of Canada. On the Ob', Yukon, and Mackenzie Rivers, gauging stations are identical to the ArcticGRO sample collection location. On the Yenisey, Lena, and Kolyma Rivers, proximate gauging stations were used, at Kyusyur, Igarka, and Kolymskoye, respectively. The effect of this modest offset, and methods for correction, have been described elsewhere[54]. Continually-updated concentration and discharge datasets are available on the ArcticGRO website. Concentration and discharge data used for this analysis (i.e., 2003 – 2019, inclusive) have been archived at the Arctic Data Center (https://doi.org/10.18739/A2VH5CK43).

Determination of constituent flux using the WRTDS Kalman approach

Determining constituent flux requires a modelling approach, because discharge data are typically available at daily (or even more refined) time steps, while concentration measurements are almost always collected much more patchily over time. We used the Weighted Regressions on Time, Discharge, and Season (WRTDS) approach to estimate constituent flux over the ArcticGRO period of record, actualized in the *EGRET* (Exploration and Graphics for RivEr Trends)[56] package in the R statistical platform[57]. This approach has been shown to provide more accurate estimates of constituent flux than other common statistical techniques used for flux estimation[58], as a result of the use of weighted regression (see below), and the removal of the requirement for homoscedastic residuals for bias correction[59]. Similar to other flux estimation techniques, the predictive equation takes the form of:

$$\ln(c) = \beta_0 + \beta_1 t + \beta_2 \ln(Q) + \beta_3 \sin(2\pi t) + \beta_4 \cos(2\pi t) + \varepsilon \quad (1)$$

where c is concentration, Q is discharge, t is time in decimal years, and ε is the unexplained variation, with the sine and cosine functions enabling seasonality within the model[30]. However, unlike most other flux modelling approaches, the coefficients $\beta_0 - \beta_4$ are not static, but are allowed to vary gradually in *Q, t* space. This is accomplished via an approach that develops a separate model for each day of the observational record by re-evaluating the relationship between concentration and time, season, and discharge, with a weighting that prioritizes samples closest in *Q, t* space to the day of estimation[59]. For

this work, we use the WRTDS-Kalman modification, which further improves upon the above-described technique by using a first order autoregressive (AR1) model to capture residual autocorrelation[60]. An assessment of measured vs. modelled daily outputs via WRTDS-Kalman is provided in Extended Data Figure 6. Daily WRTDS-Kalman flux outputs have been archived at the Arctic Data Center (https://doi.org/10.18739/A2VH5CK43).

Calculation of flow-normalized flux, and assessment of flow-normalized trends

A complication of evaluating trends in flux is that a substantial amount of variation in concentration is caused by year-to-year variation in discharge, which adds considerable noise to the time series. To assess changes in flux with year-to-year variation in discharge removed, we use the WRTDS *flow normalization* technique, which filters out the influence of inter-annual variation in streamflow. This is accomplished by creating a probability density function (pdf) of *Q* for each day of the calendar year, and producing flow-normalized concentrations and fluxes that integrates over this pdf[32]. In this way, discharge is normalized across calendar years, but intra-annual variation (i.e., seasonal variation, at a daily time step) is retained. Given the statistical complexity of this smoothing approach, we estimate uncertainty in change over the flow normalized time series using a block bootstrap technique implemented in the R package *EGRETci*, which creates a posterior mean estimate ($\hat{\pi}$) of the probability of a trend, and assesses trend likelihood as: highly likely ($\hat{\pi}$ <0.05 or >0.95) very likely ($\hat{\pi}$ 0.05-0.10 or 0.90-0.95), likely ($\hat{\pi}$ 0.10-0.33 or 0.66-0.90), or about as likely as not ($\hat{\pi}$ 0.33-0.66)[32]. Our results are provided as mean and 90% confidence interval outputs from the block bootstrap approach described in ref. [32].

Assessment of trends in annual discharge and WRTDS-Kalman constituent flux

Daily discharge and flux estimates were summed within years to generate an annual time series, and a Mann-Kendall test was used to analyze the significance of annual trends over time. Within this analysis, trend slopes were calculated using the Theil-Sen method. Trend analyses, and the calculation of slopes were conducted using the *trend* package[61] in R[57]. We report Kendall's p-value and Sen's slope in the main text, and report additional statistical outputs in Table S1.

Assessment of trends in concentration

To allow us to examine trends in concentration directly, but account for seasonal variation in concentration measurements that may skew trend detection, we used a Seasonal Kendall test[62]. This approach accounts for seasonality by calculating the Mann-Kendall statistic for each of *p* seasons directly, and then combines the test statistic for each season (S_p) to create an overall seasonal Kendall statistic (S'):

$$S' = \sum_{i=1}^{p} S_p$$

We used a modification of the original seasonal Kendall test which accounts for serial dependence by using an autogregressive moving average (ARMA) (1:1) approach[63]. We defined seasons as spring (May-June), summer (July-October) and winter (November-April), as has been previously established for the ArcticGRO dataset[54,64]. We further used a seasonal Kendall slope estimator to determine the magnitude of trends, following the Theil-Sen approach as modified for the seasonal Kendall test[62].

Data visualization

Figures 2-4 and Extended Data figures 1 and 3-5 were actualized in R[57] using *ggplot2*[65]. The correlation cluster analysis shown in Extended Data figure 2 was carried out using the function "heatmap.2" in the *gplots* package[66] in R.

Data availability

Data used for our analyses and daily Kalman outputs are provided as a fixed package at the Arctic Data Center (https://doi.org/10.18739/A2VH5CK43). More recent updates of the ArcticGRO water quality and discharge datasets can be found at the project website (www.arcticgreatrivers.org) and through the Arctic Data Center[55].

Acknowledgements

Funding for the PARTNERS program and Arctic Great Rivers Observatory has been provided via NSF grants 0229302, 0732985, 0732821, 0732522, 0732583, 1107774, 1603149, 1602680, 1602615, 1914081, 1914215, 1913888, and 1913962. This work would not have been possible without contributions from many individuals at the six ArcticGRO sampling locations, and we very gratefully acknowledge contributions from Edwin Amos, Bart Blais, Charlie Couvillion, Anya Davydova, Nicole Dion, Vladimir Efremov, Les Kutny, Ryan McLeod, Robert Myers, Alexander Pavlov, Alexander Smirnov, Mikhail Suslov, Galina Zimova, and support from the Environment and Climate Change Canada (ECCC) and Indigenous and Northern Affairs Canada (INAC) offices in Inuvik, Canada. We also would like to acknowledge that sample collection occurred within the Gwich'in Settlement Region (Mackenzie River), and on the traditional territories of the Yup'ik people (Yukon River) in North America and the Evenk people (Lena River) in Russia. Julianne Waite assisted with the creation of Figure 5. Sean Sylva, Gretchen Swarr, and Maureen Auro assisted with analyses of major and trace anion/cation data.

Author contributions

Conceived of the paper and performed data analysis: SET, RMH, JWM, RGMS, AS, FM, AIS; *Led manuscript preparation:* SET; *Initial design of the ArcticGRO (PARTNERS) program:* BJP, RMH, JWM, PAR, RGS, RMWA, LWC, VVG, SZ, AVZ; *Sample and data acquisition:* AVZ, TYG, SZ, NZ, GE, PFS, EAM, RS, MT, LSK; *Performed laboratory analyses:* AS, LS, BP-E, PR, CG, PFS; *Read and commented on the manuscript:* All authors

Corresponding author: Suzanne E. Tank (suzanne.tank@ualberta.ca)

Competing interests: The authors declare no competing interests.

Extended Data Table 1: Characteristics of the six largest Arctic watersheds.

	Watershed Area	Area at gauge	Distance to Arctic Ocean[a]	Mean discharge[b] (2003-2019)	Runoff (2003-2019)	Permafrost[c]	Continuous Permafrost[c]	Discontinuous Permafrost[c]	Tundra[d]	Forest[d]	Regulated[e]	Mean annual temperature (2003-2019)[f]	Mean annual precipitation (2003-2019)[f]	Population Density[g]
	10^6 km^2	10^6 km^2	km	km^3 y^{-1}	mm y^{-1}	(% area)	(% area)	(% area)	(% area)	(% area)	(% area)	^{o}C	mm y^{-1}	people km^{-2}
Ob'	2.99	2.95	287	409	139	26	2	4	0.1	48.2	14.6	-0.7	604	9.07
Yenisey	2.54	2.44	433 (697)	595	244	88	33	11	0.5	67.9	50.5	-4.4	619	2.85
Lena	2.46	2.43	754 (211)	599	247	99	79	11	1.2	62.5	7.2	-8.9	548	0.45
Kolyma	0.65	0.53	120 (283)	108	205	100	100	0	3.2	16.7	18.9	-10.7	546	0.2
Yukon	0.83	0.83	200	211	254	99	23	66	0.1	68.4	0.0	-4.8	571	0.17
Mackenzie	1.78	1.68	260	295	176	82	16	29	0.0	74.2	4.3	-3.6	547	0.25
Sum	11.25	--		2,217	--	--	--	--	--	--	--	--	--	--
Pan-Arctic	16.8[h]	--	--	~3710[i]	~220	--	--	--	--	--	--	--	--	--

[a] Distance from the water chemistry station (discharge gauge) to the Arctic Ocean, including transit distance through river mouth Deltas. Where only one value is presented, water chemistry and discharge data collection are co-located. Data for Russian rivers are from the Hydrometeorological Service of the USSR[67]. Data for North American rivers are estimated from Google Earth.

[b] Mean annual discharge over the study period

[c] From Holmes et al. (2013)[68]. Permafrost extent and classification from the International Permafrost Association's Circum-Arctic Map of Permafrost and Ground Ice Conditions.

[d] Vegetation classes from the 20-class GLDAS/NOAH product[69], based on a 30 arc second MODIS vegetation data that uses a modified IGBP classification scheme. Tundra is the sum of mixed and bare ground tundra. Forest is the sum of evergreen, deciduous, and mixed forest, and wooded tundra.

[e] Regulated area at the end of the study period, from Lehner et al. (2011)[70]. Includes impoundments that were completed on the Kolyma (2013) and Yenisey (2012) rivers during the ArcticGRO period of analysis.

[f] Mean annual temperature and precipitation from the MERRA2 reanalysis product[71].

[g] Population density from the Center for International Earth Science Information Network (2018)[72] gridded population of the world.

[h] Watershed area of 16.8 x 10^6 km^2 corresponds to the area demarcated in Figure 1, which does not include drainage to Hudson Bay. The pan-Arctic watershed including Hudson Bay, but excluding the Greenland Ice Cap, covers an area of 22.4 x 10^6 km^2 (from Lammers et al. 2001[73])

[i] Estimate derived from Shiklomanov et al. 2021[22], for the period covering 1980-2018

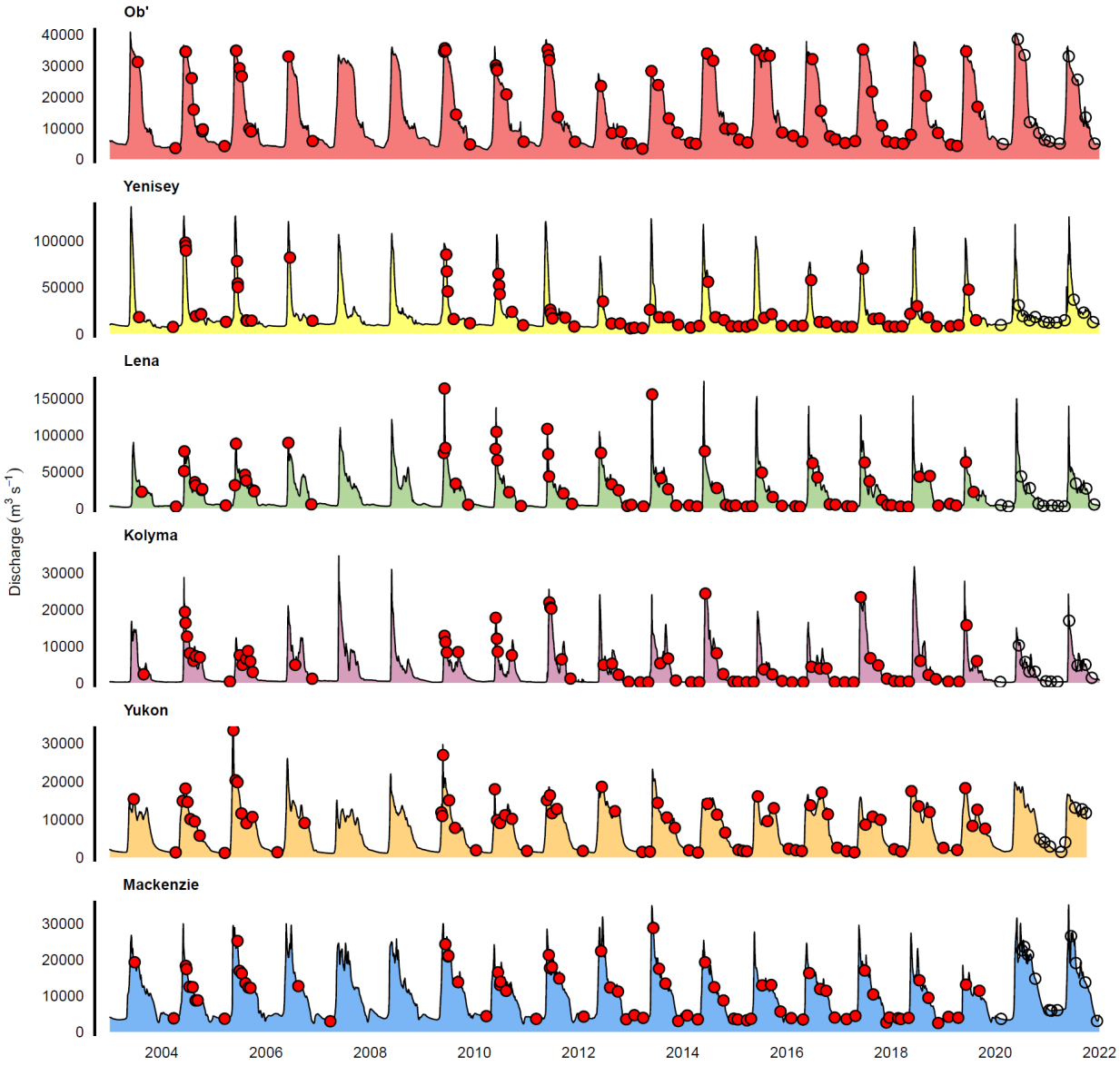

Extended Data Figure 1: Time-series of discharge and concentration measurements across the six Arctic Great Rivers. Discharge is shown as a continuous time-series for all rivers. Dates of sample collection for concentration measurements used in this analysis are shown with red circles; clear circles indicate ongoing data collection.

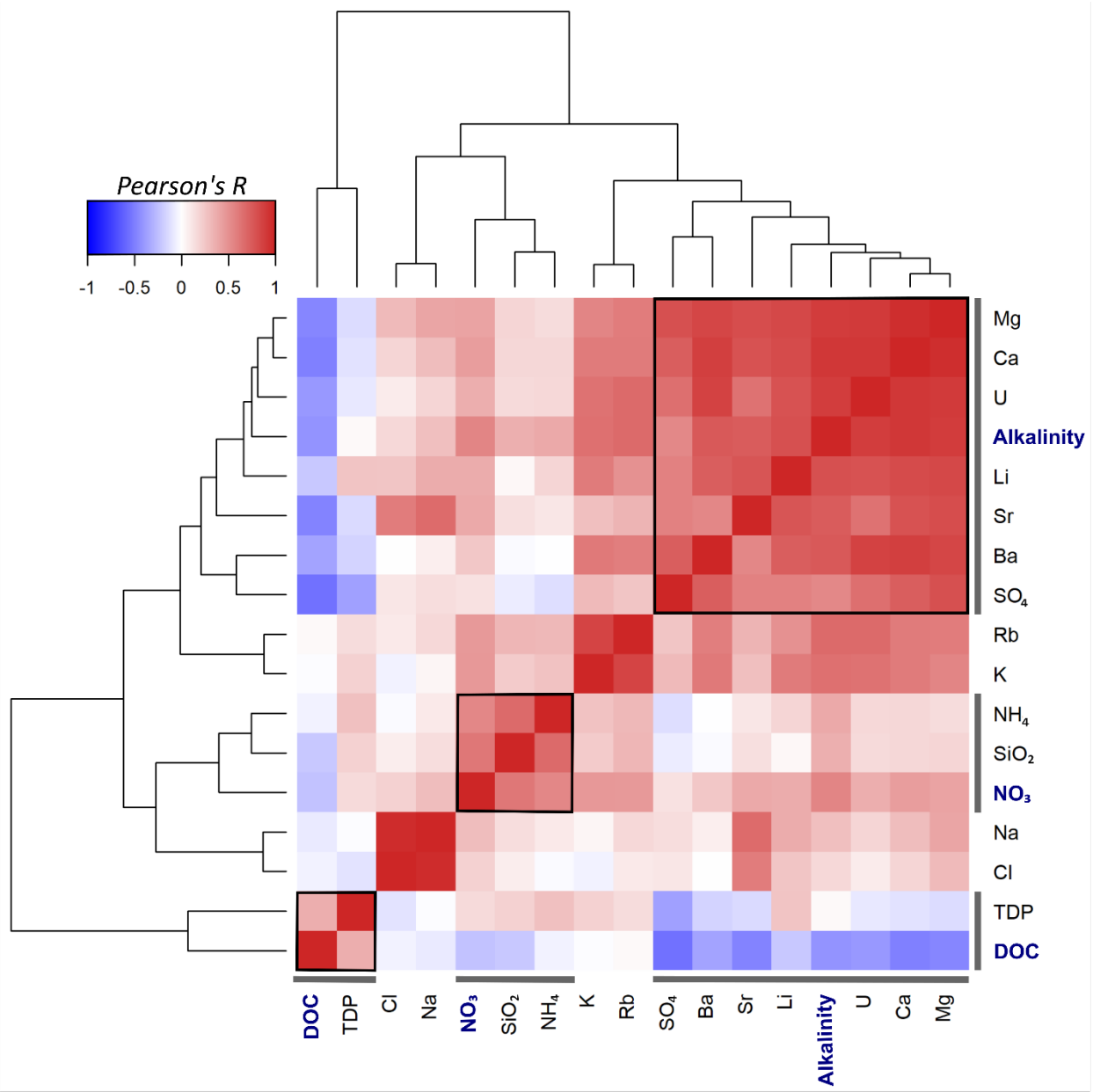

Extended Data Figure 2: A cluster heatmap illustrating correlation between constituents for the full ArcticGRO dataset. Shading indicates the Pearson correlation coefficient, which was used as the distance metric for hierarchical clustering. Focal constituents (alkalinity, nitrate [NO_3-N], and dissolved organic carbon [DOC]) are bolded in blue. Black boxes within the correlation plot and grey shading along axes indicate clusters associated with each focal constituent.

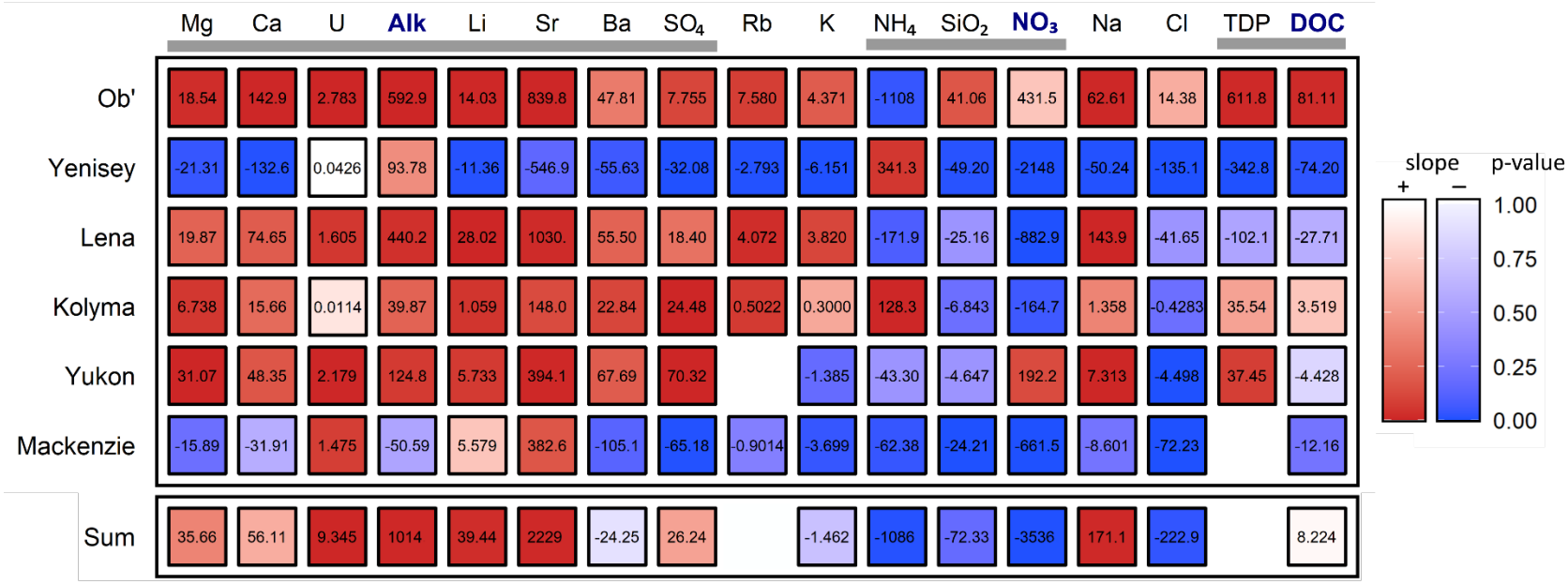

Extended Data Figure 3: Annual trends in constituent flux across the full ArcticGRO dataset, for each of the six great Arctic rivers. Trend analysis is via a Mann-Kendall analysis; the Thiel-Sen slope (numerical value) and p-value of the trend analysis (shading) are shown. Corresponding trends in concentration are provided in Extended Data Figure 5. Grey bars illustrate groupings from Extended Data Figure 2. Units (Gg y^{-1} or Mg y^{-1}) are provided in Table S1.

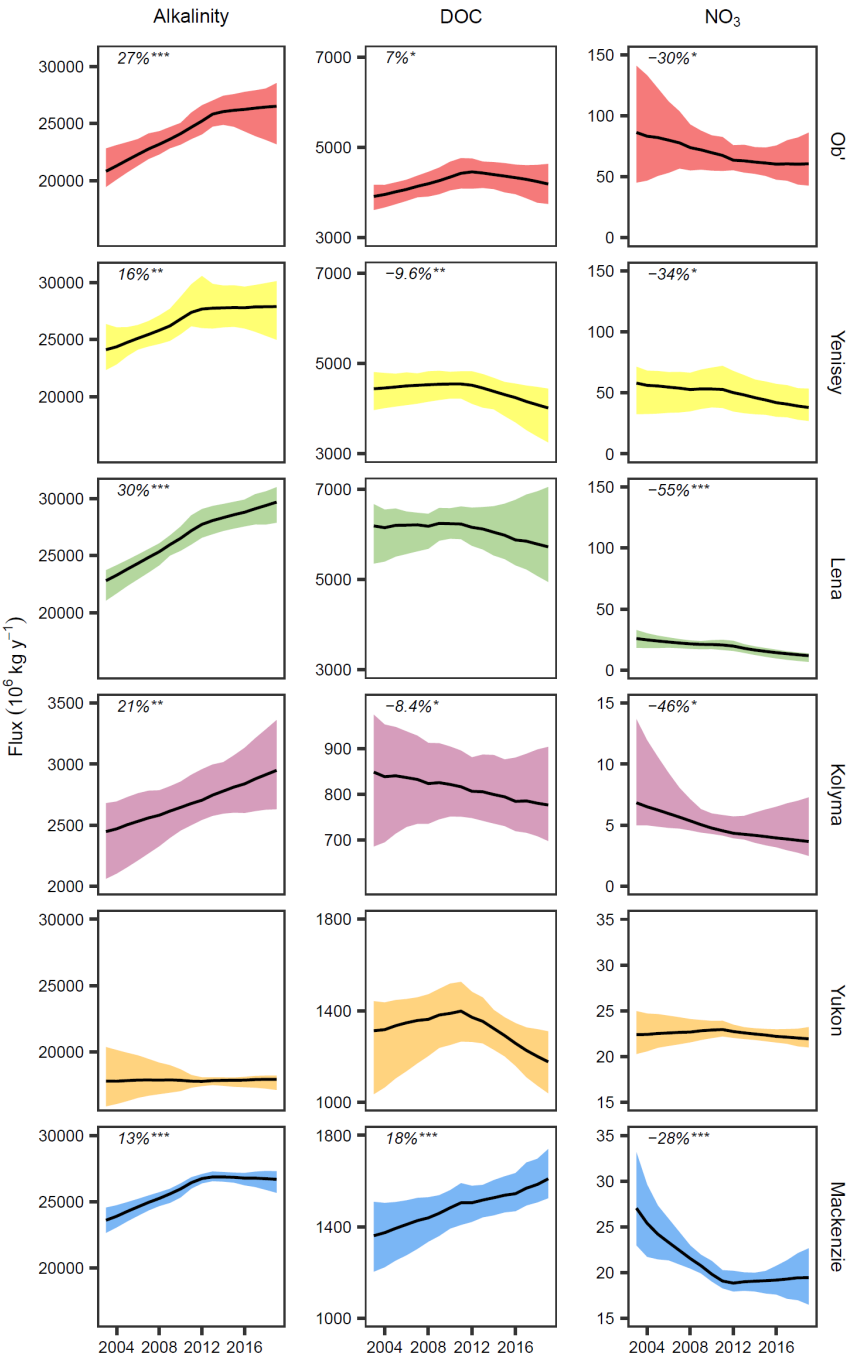

Extended Data Figure 4: Flow-weighted trends in annual constituent flux for the three focal constituents (alkalinity, dissolved organic carbon [DOC], and nitrate [NO_3-N], for each of the six Great Arctic rivers. The solid line indicates the mean, and shading indicates 90% confidence interval from the block bootstrap analysis. Asterisks indicate trends that are: ***highly likely (posterior mean estimate $\hat{\pi}$ <0.05 or >0.95); **very likely ($\hat{\pi}$ 0.05-0.10 or 0.90-0.95); or *likely ($\hat{\pi}$ 0.10-0.33 or 0.66-0.90), with percentage change in constituent flux indicated for the period of record. Where no percentage change is shown, trends were assessed to be about as likely as not ($\hat{\pi}$ 0.33-0.66).

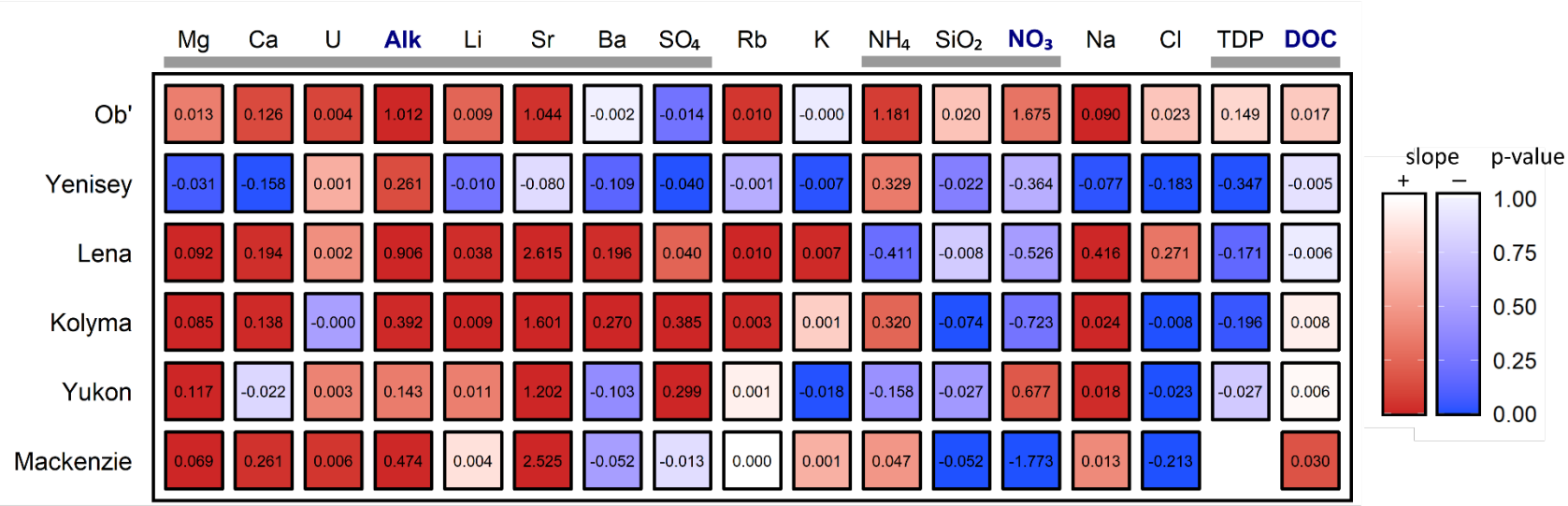

Extended Data Figure 5: Trends for constituent concentration across the full ArcticGRO dataset, for each of the six great Arctic rivers. Trend analysis is via a seasonal Mann-Kendall analysis; the Thiel-Sen slope (numerical value) and p-value of the trend analysis (shading) are shown. Corresponding trends in constituent flux are provided in Extended Data Figure 3. Grey bars illustrate groupings from Extended Data Figure 2. Units (mg L^{-1} y^{-1} or µg L^{-1} y^{-1}) are provided in Table S2.

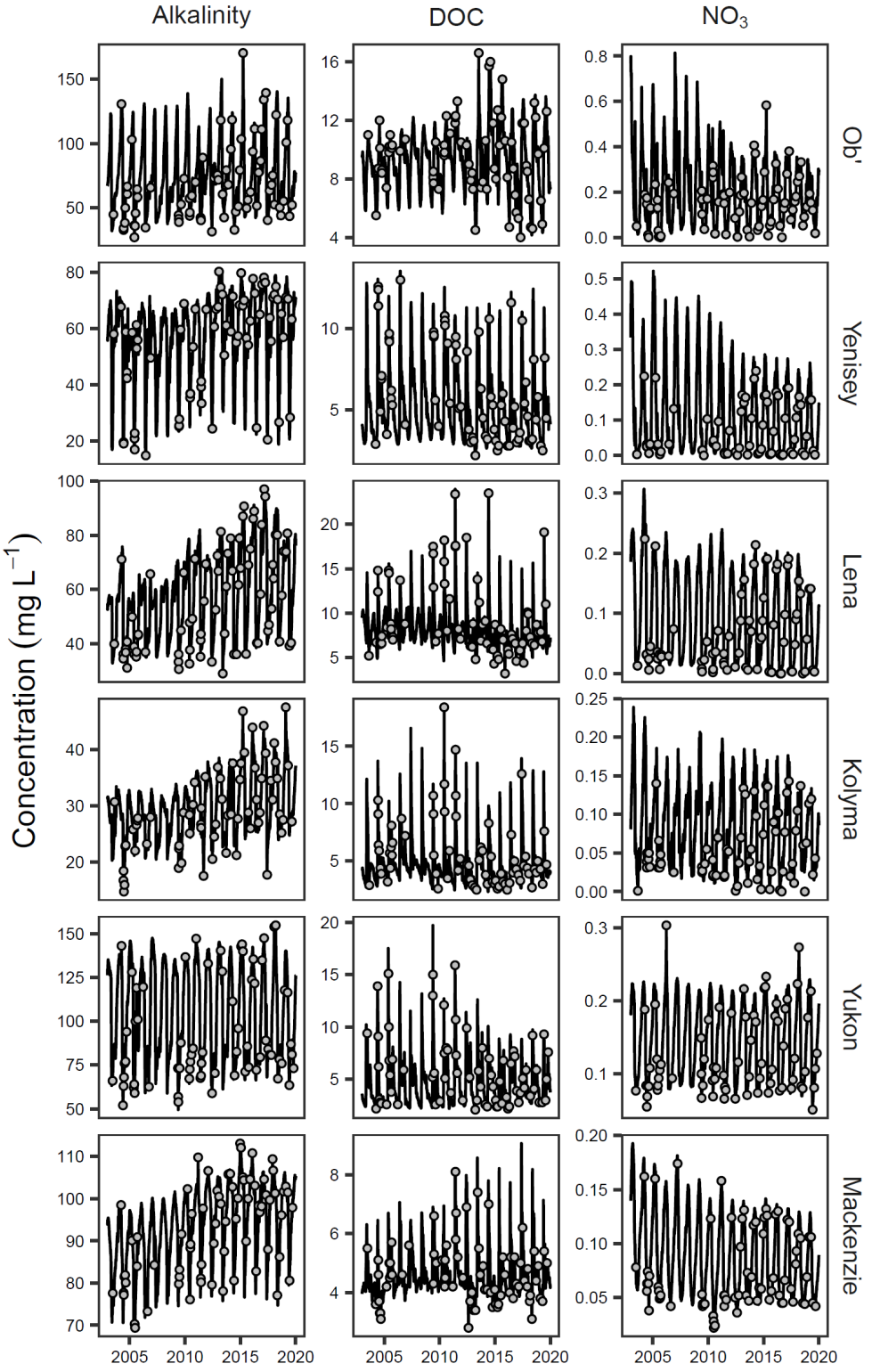

447

448 **Extended Data Figure 6**: Measured vs. modelled concentrations of the focal constituent suite, for each
449 of the six great Arctic rivers. Circles indicate true concentration measurements; lines indicate outputs
450 from the WRTDS-Kalman model.

References

1 Carmack, E. C. *et al.* Freshwater and its role in the Arctic Marine System: Sources, disposition, storage, export, and physical and biogeochemical consequences in the Arctic and global oceans. *J. Geophys. Res.-Biogeosci.* **121**, 675-717, doi:https://doi.org/10.1002/2015JG003140 (2016).

2 Tank, S. E. *et al.* A land-to-ocean perspective on the magnitude, source and implication of DIC flux from major Arctic rivers to the Arctic Ocean. *Global Biogeochem. Cycles* **26**, GB4018, doi:10.1029/2011GB004192 (2012).

3 Dunton, K. H., Weingartner, T. & Carmack, E. C. The nearshore western Beaufort Sea ecosystem: Circulation and importance of terrestrial carbon in arctic coastal food webs. *Progress in Oceanography* **71**, 362–378 (2006).

4 Terhaar, J., Lauerwald, R., Regnier, P., Gruber, N. & Bopp, L. Around one third of current Arctic Ocean primary production sustained by rivers and coastal erosion. *Nat. Commun.* **12**, 169, doi:10.1038/s41467-020-20470-z (2021).

5 McClelland, J. W., Holmes, R. M., Dunton, K. H. & Macdonald, R. W. The Arctic Ocean estuary. *Estuar. Coast.* **35**, 353–368, doi:10.1007/s12237-010-9357-3 (2012).

6 Previdi, M., Smith, K. L. & Polvani, L. M. Arctic amplification of climate change: a review of underlying mechanisms. *Environ. Res. Lett.* **16**, 093003, doi:10.1088/1748-9326/ac1c29 (2021).

7 Peterson, B. J. *et al.* Increasing river discharge to the Arctic Ocean. *Science* **298**, 2171-2173 (2002).

8 McClelland, J. W., Dery, S. J., Peterson, B. J., Holmes, R. M. & Wood, E. F. A pan-arctic evaluation of changes in river discharge during the latter half of the 20th century. *Geophys. Res. Lett.* **33**, L06715, doi:10.1029/2006GL025753 (2006).

9 Rawlins, M. A. *et al.* Analysis of the Arctic system for freshwater cycle intensification: Observations and expectations. *J. Clim.* **23**, 5715-5737, doi:doi:10.1175/2010JCLI3421.1 (2010).

10 Raymond, P. A. *et al.* Flux and age of dissolved organic carbon exported to the Arctic Ocean: A carbon isotopic study of the five largest Arctic rivers. *Glob. Biogeochem. Cycles* **21**, GB4011, doi:10.1029/2007GB002934 (2007).

11 Gómez-Gener, L., Hotchkiss, E. R., Laudon, H. & Sponseller, R. A. Integrating Discharge-concentration dynamics across carbon forms in a boreal landscape. *Water Resour. Res.* **57**, e2020WR028806, doi:https://doi.org/10.1029/2020WR028806 (2021).

12 Toohey, R. C., Herman-Mercer, N. M., Schuster, P. F., Mutter, E. A. & Koch, J. C. Multidecadal increases in the Yukon River Basin of chemical fluxes as indicators of changing flowpaths, groundwater, and permafrost. *Geophys. Res. Lett.* **43**, 12,120-112,130, doi:10.1002/2016gl070817 (2016).

13 Shogren, A. J. *et al.* Revealing biogeochemical signatures of Arctic landscapes with river chemistry. *Sci Rep* **9**, 12894, doi:10.1038/s41598-019-49296-6 (2019).

14 Gabysheva, O. I., Gabyshev, V. A. & Barinova, S. Influence of the active layer thickness of permafrost in eastern Siberia on the river discharge of nutrients into the Arctic Ocean. *Water* **14**, 84 (2022).

15 Tape, K., Sturm, M. & Racine, C. The evidence for shrub expansion in Northern Alaska and the Pan-Arctic. *Global Change Biol.* **12**, 686-702, doi:10.1111/j.1365-2486.2006.01128.x (2006).

16 Reay, D. S., Nedwell, D. B., Priddle, J. & Ellis-Evans, J. C. Temperature dependence of inorganic nitrogen uptake: reduced affinity for nitrate at suboptimal temperatures in both algae and bacteria. *Appl. Environ. Microb.* **65**, 2577-2584, doi:10.1128/AEM.65.6.2577-2584.1999 (1999).

17 Salazar, A., Rousk, K., Jónsdóttir, I. S., Bellenger, J.-P. & Andrésson, Ó. S. Faster nitrogen cycling and more fungal and root biomass in cold ecosystems under experimental warming: a meta-analysis. *Ecology* **101**, e02938, doi:https://doi.org/10.1002/ecy.2938 (2020).

18 Wickland, K. P. *et al.* Biodegradability of dissolved organic carbon in the Yukon River and its tributaries: Seasonality and importance of inorganic nitrogen. *Glob. Biogeochem. Cycles* **26**, GB0E03, doi:10.1029/2012gb004342 (2012).
19 Box, J. E. *et al.* Key indicators of Arctic climate change: 1971–2017. *Environ. Res. Lett.* **14**, 045010, doi:10.1088/1748-9326/aafc1b (2019).
20 Maavara, T. *et al.* River dam impacts on biogeochemical cycling. *Nature Reviews Earth & Environment* **1**, 103-116, doi:10.1038/s43017-019-0019-0 (2020).
21 Zolkos, S. *et al.* Multidecadal declines in particulate mercury and sediment export from Russian rivers in the pan-Arctic basin. *Proc. Natl. Acad. Sci. USA* **119**, e2119857119, doi:doi:10.1073/pnas.2119857119 (2022).
22 Shiklomanov, A. *et al.* in *Arctic Hydrology, Permafrost and Ecosystems* (eds Daqing Yang & Douglas L. Kane) 703-738 (Springer International Publishing, 2021).
23 Bergen, K. M. *et al.* Long-term trends in anthropogenic land use in Siberia and the Russian Far East: a case study synthesis from Landsat. *Environ. Res. Lett.* **15**, 105007, doi:10.1088/1748-9326/ab98b7 (2020).
24 Aas, W. *et al.* Global and regional trends of atmospheric sulfur. *Sci Rep* **9**, 953, doi:10.1038/s41598-018-37304-0 (2019).
25 Slaveykova, V. I. Biogeochemical dynamics research in the Anthropocene. *Frontiers in Environmental Science* **7**, doi:10.3389/fenvs.2019.00090 (2019).
26 Vonk, J. E., Tank, S. E. & Walvoord, M. A. Integrating hydrology and biogeochemistry across frozen landscapes. *Nat. Commun.* **10**, 5377 (2019).
27 Opfergelt, S. The next generation of climate model should account for the evolution of mineral-organic interactions with permafrost thaw. *Environ. Res. Lett.* **15**, 091003, doi:10.1088/1748-9326/ab9a6d (2020).
28 Shakil, S., Tank, S. E., Vonk, J. E. & Zolkos, S. Low biodegradability of particulate organic carbon mobilized from thaw slumps on the Peel Plateau, NT, and possible chemosynthesis and sorption effects. *Biogeosciences* **19**, 1871-1890, doi:10.5194/bg-19-1871-2022 (2022).
29 Tank, S. E. *et al.* Landscape matters: Predicting the biogeochemical effects of permafrost thaw on aquatic networks with a state factor approach. *Permafrost Periglac.* **31**, 358-370, doi:https://doi.org/10.1002/ppp.2057 (2020).
30 Hirsch, R. M., Moyer, D. L. & Archfield, S. A. Weighted regressions on time, discharge, and season (WRTDS), with an application to Chesapeake Bay river inputs. *JAWRA Journal of the American Water Resources Association* **46**, 857-880, doi:https://doi.org/10.1111/j.1752-1688.2010.00482.x (2010).
31 Terhaar, J., Orr, J. C., Ethé, C., Regnier, P. & Bopp, L. Simulated Arctic Ocean response to doubling of riverine carbon and nutrient Delivery. *Glob. Biogeochem. Cycles* **33**, 1048-1070, doi:https://doi.org/10.1029/2019GB006200 (2019).
32 Hirsch, R. M., Archfield, S. A. & De Cicco, L. A. A bootstrap method for estimating uncertainty of water quality trends. *Environmental Modelling & Software* **73**, 148-166, doi:https://doi.org/10.1016/j.envsoft.2015.07.017 (2015).
33 Kokelj, S. V. & Jorgenson, M. T. Advances in thermokarst research. *Permafrost Periglac.* **24**, 108-119, doi:10.1002/ppp.1779 (2013).
34 Littlefair, C. A., Tank, S. E. & Kokelj, S. V. Retrogressive thaw slumps temper dissolved organic carbon delivery to streams of the Peel Plateau, NWT, Canada. *Biogeosciences* **14**, 5487-5505, doi:10.5194/bg-14-5487-2017 (2017).
35 Frey, K. E. & McClelland, J. W. Impacts of permafrost degradation on Arctic river biogeochemistry. *Hydrol. Process.* **23**, 169-182, doi:10.1002/hyp.7196 (2009).

36 Keller, K., Blum, J. D. & Kling, G. W. Stream geochemistry as an indicator of increasing permafrost thaw depth in an arctic watershed. *Chem. Geol.* **273**, 76-81 (2010).

37 Zolkos, S., Tank, S. E. & Kokelj, S. V. Mineral weathering and the permafrost carbon-climate feedback. *Geophys. Res. Lett.* **45**, 9623-9632, doi:doi:10.1029/2018GL078748 (2018).

38 Berner, R. A. The carbon cycle and CO_2 over Phanerozoic time: the role of land plants. *Philos. Trans. R. Soc. B-Biol. Sci.* **353**, 75-81, doi:10.1098/rstb.1998.0192 (1998).

39 Beaulieu, E., Godderis, Y., Donnadieu, Y., Labat, D. & Roelandt, C. High sensitivity of the continental-weathering carbon dioxide sink to future climate change. *Nature Clim. Change* **2**, 346-349, doi:10.1038/nclimate1419 (2012).

40 Vonk, J. E. *et al.* High biolability of ancient permafrost carbon upon thaw. *Geophys. Res. Lett.* **40**, 2689-2693, doi:10.1002/grl.50348 (2013).

41 Finstad, A. G. *et al.* From greening to browning: Catchment vegetation development and reduced S-deposition promote organic carbon load on decadal time scales in Nordic lakes. *Sci Rep* **6**, 31944, doi:10.1038/srep31944 (2016).

42 Moore, T. R., Paré, D. & Boutin, R. Production of dissolved organic carbon in Canadian forest soils. *Ecosystems* **11**, 740-751, doi:10.1007/s10021-008-9156-x (2008).

43 Drake, T. W. *et al.* The Ephemeral signature of permafrost carbon in an Arctic fluvial network. *J. Geophys. Res.-Biogeosci.* **123**, 1475-1485, doi:10.1029/2017jg004311 (2018).

44 Hicks Pries, C. E., McLaren, J. R., Smith Vaughn, L., Treat, C. & Voigt, C. in *Multi-scale Biogeochemical Processes in Soil Ecosystems: Critical Reactions and Resilience to Climate Change* (eds Y. Yu Yang, M. Keiluweit, N. Senesi, & B. Xing) (John Wiley & Sons, Inc., 2022).

45 Kicklighter, D. W. *et al.* Insights and issues with simulating terrestrial DOC loading of Arctic river networks. *Ecol. Appl.* **23**, 1817-1836, doi:https://doi.org/10.1890/11-1050.1 (2013).

46 Burke, A. *et al.* Sulfur isotopes in rivers: Insights into global weathering budgets, pyrite oxidation, and the modern sulfur cycle. *Earth Planet. Sc. Lett.* **496**, 168-177, doi:https://doi.org/10.1016/j.epsl.2018.05.022 (2018).

47 Lacroix, F., Ilyina, T. & Hartmann, J. Oceanic CO_2 outgassing and biological production hotspots induced by pre-industrial river loads of nutrients and carbon in a global modeling approach. *Biogeosciences* **17**, 55-88, doi:10.5194/bg-17-55-2020 (2020).

48 Lewis, K. M., van Dijken, G. L. & Arrigo, K. R. Changes in phytoplankton concentration now drive increased Arctic Ocean primary production. *Science* **369**, 198-202, doi:doi:10.1126/science.aay8380 (2020).

49 Chang, B. X. & Devol, A. H. Seasonal and spatial patterns of sedimentary denitrification rates in the Chukchi sea. *Deep Sea Research Part II: Topical Studies in Oceanography* **56**, 1339-1350, doi:https://doi.org/10.1016/j.dsr2.2008.10.024 (2009).

50 Dutkiewicz, S. *et al.* Impact of ocean acidification on the structure of future phytoplankton communities. *Nature Climate Change* **5**, 1002-1006, doi:10.1038/nclimate2722 (2015).

51 McClelland, J. W., Stieglitz, M., Pan, F., Holmes, R. M. & Peterson, B. J. Recent changes in nitrate and dissolved organic carbon export from the upper Kuparuk River, North Slope, Alaska. *J. Geophys. Res.-Biogeosci.* **112**, G04S60, doi:10.1029/2006JG000371 (2007).

52 Kendrick, M. R. *et al.* Linking permafrost thaw to shifting biogeochemistry and food web resources in an Arctic river. *Global Change Biol.* **24**, 5738-5750, doi:10.1111/gcb.14448 (2018).

53 Davis, B. E. A guide to the proper selection and use of federally approved sediment and water-quality samplers. Report No. 2005-1087, (2005).

54 Holmes, R. M. *et al.* Seasonal and annual fluxes of nutrients and organic matter from large rivers to the Arctic Ocean and surrounding seas. *Estuar. Coast.* **35**, 369-382, doi:10.1007/s12237-011-9386-6 (2012).

55 Holmes, R. M., McClelland, J., Tank, S., Spencer, R. & Shiklomanov, A. Arctic Great Rivers Observatory IV Biogeochemistry and Discharge Data: 2020-2024. Arctic Data Center. doi:10.18739/A2XW47X7D (2022).
56 Hirsch, R. M. & De Cicco, L. A. User guide to Exploration and Graphics for RivEr Trends (EGRET) and dataRetrieval: R packages for hydrologic data. Report No. 4-A10, 104 (Reston, VA, 2015).
57 R Core Team. (R Foundation for Statistical Computing, Vienna, Austria, 2022).
58 Lee, C. J. *et al.* An evaluation of methods for estimating decadal stream loads. *J. Hydrol.* **542**, 185-203, doi:https://doi.org/10.1016/j.jhydrol.2016.08.059 (2016).
59 Hirsch, R. M. Large biases in regression-based constituent flux estimates: Causes and diagnostic tools. *JAWRA Journal of the American Water Resources Association* **50**, 1401-1424, doi:https://doi.org/10.1111/jawr.12195 (2014).
60 Zhang, Q. & Hirsch, R. M. River Water-quality concentration and flux estimation can be improved by accounting for serial correlation through an autoregressive model. *Water Resour. Res.* **55**, 9705-9723, doi:https://doi.org/10.1029/2019WR025338 (2019).
61 trend: Non-Parametric Trend Tests and Change-Point Detection. R package version 1.1.4. (2020).
62 Hirsch, R. M., Slack, J. R. & Smith, R. A. Techniques of trend analysis for monthly water quality data. *Water Resour. Res.* **18**, 107-121, doi:https://doi.org/10.1029/WR018i001p00107 (1982).
63 Hirsch, R. M. & Slack, J. R. A Nonparametric trend test for seasonal data with serial dependence. *Water Resour. Res.* **20**, 727-732, doi:https://doi.org/10.1029/WR020i006p00727 (1984).
64 McClelland, J. W. *et al.* Particulate organic carbon and nitrogen export from major Arctic rivers. *Glob. Biogeochem. Cycles* **30**, 629-643, doi:10.1002/2015gb005351 (2016).
65 Wickham, H. *ggplot2: Elegant Graphics for Data Analysis*. (Springer-Verlag, 2016).
66 Warnes, G. R. *et al.* gplots: Various R Programming Tools for Plotting Data. R package version 3.1.3. https://CRAN.R-project.org/package=gplots. (2022).
67 *The Resources of Surface Waters of the USSR. Hydrological Knowledge.*, Vol. 15, 16, 17, 19 (Gidrometeoizdat, 1965-1969).
68 Holmes, R. M. *et al.* in *Climatic Change and Global Warming of Inland Waters: Impacts and Mitigation for Ecosystems and Societies* (eds C.R. Goldman, M. Kumagi, & R.D. Robarts) (Wiley, 2013).
69 Rodell, M. *et al.* The global land data assimilation system. *Bulletin of the American Meteorological Society* **85**, 381-394 (2004).
70 Lehner, B. *et al.* High-resolution mapping of the world's reservoirs and dams for sustainable river-flow management. *Front. Ecol. Environ.* **9**, 494-502, doi:https://doi.org/10.1890/100125 (2011).
71 Gelaro, R. *et al.* The modern-era retrospective analysis for research and applications, Version 2 (MERRA-2). *J. Clim.* **30**, 5419-5454, doi:10.1175/jcli-d-16-0758.1 (2017).
72 Center for International Earth Science Information Network - CIESIN - Columbia University. (NASA Socioeconomic Data and Applications Center (SEDAC), Palisades, New York, 2018).
73 Lammers, R. B., Shiklomanov, A. I., Vorosmarty, C. J., Fekete, B. M. & Peterson, B. J. Assessment of contemporary Arctic river runoff based on observational discharge records. *J. Geophys. Res.-Atmos.* **106**, 3321-3334 (2001).

Supplementary Files

This is a list of supplementary files associated with this preprint. Click to download.

- AGROLongTermChangeSupplement20230130.pdf